NEUTRON ENERGY SPECTRUM RECONSTRUCTION METHOD

BASED FOR HTR REACTOR CALCULATIONS

A Thesis
Presented to
The Academic Faculty

by

Zhan Zhang

In Partial Fulfillment
of the Requirements for the Degree
Master of Science in Nuclear and Radiological Engineering in the
School of Mechanical Engineering

Georgia Institute of Technology
August 2011

NEUTRON ENERGY SPECTRUM RECONSTRUCTION METHOD

BASED FOR HTR REACTOR CALCULATIONS

Approved by:

Dr. Farzad Rahnema, Advisor
School of Mechanical Engineering
Georgia Institute of Technology

Dr. Dingkang Zhang
School of Mechanical Engineering
Georgia Institute of Technology

Dr. Bojan Petrovic
School of Mechanical Engineering
Georgia Institute of Technology

Date Approved: June 17, 2011

[To Mom and Dad]

ACKNOWLEDGEMENTS

I would like to express my deepest appreciation to my advisor, Dr. Rahnema, for his guidance, support and patience over the past several years. I would also like to thank Dr. Zhang, for providing invaluable suggestions on my research, as well as Dr. Petrovic, for serving on my reading committee.

The contents and scope of this thesis were suggested by Dr. Abderrafi M. Ougouag of Idaho National Laboratory (INL). The author is grateful for that input.

This work was supported by the Deep Burn Project from the INL, and was conducted under contract 00100121. This support is gratefully acknowledged.

I would like to especially thank my wife, Yu Wang, for her continual love, encouragement and support in my life. Lastly, I would like to thank my parents, for their unlimited understanding and life-long support.

TABLE OF CONTENTS

	Page
ACKNOWLEDGEMENTS	iv
LIST OF TABLES	vii
LIST OF FIGURES	ix
SUMMARY	x
CHAPTER	
1 Introduction	1
2 Theory	3
2.1 Problem Definition	3
2.2 Energy Reconstruction Methods	4
2.3 Response Method	6
3 HTR Test Problem and Sensitivity Analysis	9
3.1 Problem Description	9
3.2 Sensitivity Analysis	12
4 Results	18
4.1 Reconstructed Energy Spectrum Results	19
4.2. Absorption Cross Section Results	25
5 PBR Test Problem	28
5.1 Problem Description	28
5.2 Reconstructed Energy Spectrum	29
6 Conclusions	31
APPENDIX A: B-spline Bases	32
APPENDIX B: Group Boundaries	34

APPENDIX C: Collective Error Definition 36

APPENDIX D: BP Absorption Cross Section Errors in HTR problem 37

REFERENCES 43

LIST OF TABLES

Page

Table 3.1: Absorption cross section errors introduced by different group numbers of the BP pin cell boundary conditions (single block energy spectra) 13

Table 3.2: Absorption cross section errors introduced by different angular approximations of the BP pin cell boundary conditions (single block energy spectra) 14

Table 3.3: Collective errors in absorption cross sections introduced by different angular approximations of the BP pin cell boundary conditions (reference energy spectra for all the102 BP pins) 14

Table 3.4: Collective errors in BP absorption cross sections calculated by single block model 16

Table 4.1: Errors in single block spectra and reconstructed spectra in the controlled core 20

Table 4.2: Collective errors in single block spectra and reconstructed spectra in the controlled core 22

Table 4.3: Errors in single block spectra and reconstructed spectra in the uncontrolled core 23

Table 4.4: Collective errors in single block spectra and reconstructed spectra in the uncontrolled core 24

Table 4.5: Absorption cross section errors for BP pin # 2 in fuel block 4 26

Table 4.6: Absorption rate errors for fuel block 4 26

Table 4.7: Collective errors in absorption rates for all BP pins in the whole core 27

Table 5.1: Collective errors in reconstructed energy spectra for PBR problem (33G) 29

Table 5.2: Collective errors in reconstructed energy spectra for PBR problem (71G) 30

Table B.1: Upper boundaries of energy group structures in the HTR test problem 34

Table B.2: Upper boundaries of energy group structures in the PBR test problem 35

Table D.1: Absorption cross sections and errors in fuel block 4 of the controlled core 37

Table D.2: Collective errors in absorption cross sections and absorption rates of BP pins in three BP categories in the controlled core 39

Table D.3: Absorption cross sections and errors in fuel block 4 of the controlled core 40

Table D.4: Collective errors in absorption cross sections and absorption rates of BP pins in three BP categories in the uncontrolled core 42

LIST OF FIGURES

Page

Figure 2.1: Whole core, single block and single BP cell model of prismatic HTR 4

Figure 3.1: BP number indexing and detailed geometry in the fuel block 10

Figure 3.2: Whole core layout and fuel block indexing 10

Figure 3.3: “Typical” spectra for three categories in the controlled core 11

Figure 4.1: Flowchart of the test process 18

Figure 4.2: Energy spectrum reconstruction for BP pin #2 in fuel block 4 of the controlled core 20

Figure 5.1: Layout of the PBR test problem with azimuthal symmetry 28

Figure A.1: Cubic B-spline bases 33

SUMMARY

In the deep burn research of Very High Temperature Reactor (VHTR), it is desired to make an accurate estimation of absorption cross sections and absorption rates in burnable poison (BP) pins. However, in traditional methods, multi-group cross sections are generated from single bundle calculations with specular reflection boundary condition, in which the energy spectral effect in the core environment is not taken into account. This approximation introduces errors to the absorption cross sections especially for BPs neighboring reflectors and control rods.

In order to correct the BP absorption cross sections in whole core diffusion calculations, energy spectrum reconstruction (ESR) methods have been developed to reconstruct the fine group spectrum (and in-core continuous energy spectrum). Then, using the reconstructed spectrum as boundary condition, a BP pin cell local transport calculation serves an imbedded module within the whole core diffusion code to iteratively correct the BP absorption cross sections for improved results.

The ESR methods were tested in a 2D prismatic High Temperature Reactor (HTR) problem. The reconstructed fine-group spectra have shown good agreement with the reference spectra. Comparing with the cross sections calculated by single block calculation with specular reflection boundary conditions, the BP absorption cross sections are effectively improved by ESR methods. A preliminary study was also performed to extend the ESR methods to a 2D Pebble Bed Reactor (PBR) problem. The results demonstrate that the ESR can reproduce the energy spectra on the fuel-outer reflector interface accurately.

CHAPTER 1
INTRODUCTION

In nuclear reactor simulations, whole core calculations are commonly performed using diffusion theory with approximate coarse group cross sections. These cross sections are usually generated by single bundle/block calculations with approximate boundary conditions such as infinite medium (full specular reflection) which may not be representative of the core environment. This is particularly true in VHTR related calculations. For VHTRs, with higher heterogeneity and harder energy spectra, the energy spectral effects are more significant than those in LWR cores. Significant errors are introduced to the cross sections when traditional methods do not take into account the core environment energy spectral effects. As a result, cross sections generated with the single block calculation should be corrected for core environmental effects within the core calculation.

In the deep burn research of VHTR, it is desired to obtain accurate absorption cross sections in BP pins, especially for those neighboring reflectors or control rods, because their energy spectra are greatly influenced by the neighboring lattices. It has been observed in this study that the errors in the absorption cross sections of BP pins obtained from single block calculations are up to 10%. The errors manifest themselves and the necessity of reducing the errors caused by the approximation is self-evident.

In this thesis, new energy spectrum reconstruction (ESR) methods were developed to correct the BP pin cross sections within the whole core diffusion calculation. The ESR methods reconstructed energy spectra by modulating the fine group “typical” spectra with coarse group spectra obtained from whole core calculations. The reconstructed spectra were used as boundary conditions to solve a local BP pin cell transport problem by the response method (Forget et al. 2004), in order to generate BP absorption cross sections, which take into account of the core environment energy spectral effects.

The thesis is organized as following. Chapter 2 derives the theory of ESR methods and the response method. The next chapter describes the 2D prismatic HTR test problem and performs sensitive analysis. In Chapter 4, the reconstructed spectra, BP absorption cross sections and absorption rates are analyzed. A preliminary study is performed to apply the ESR methods in a PBR test problem in Chapter 5. Then, the thesis concludes with the main findings from the test problems examining the ESR methods, as elaborated in the last chapter.

CHAPTER 2
THEORY

2.1. Problem Definition

The purpose of the ESR methods is to reconstruct fine-group (or continuous energy) spectra from coarse group spectra which are provided by whole-core diffusion calculations. The reconstructed energy spectra are then used to perform local fine-group transport calculations to improve the whole-core coarse-group diffusion solutions. The ESR methods assume that there exists a “typical” fine group spectrum (or “typical” spectra) that can represent core environment and can be used to satisfy the following requirements: (1) the reconstructed spectrum must be as close as possible to the typical spectrum and (2) the reconstructed spectrum must preserve the coarse-group spectrum. The typical spectrum is based on engineering judgment; e.g., taken from an existing whole core calculation that can broadly represent many different configurations of the same reactor types.

In the prismatic HTR test problem, preliminary sensitivity analyses indicate that the BP absorption cross sections obtained via single block calculations fail to take into account the core energy spectrum environment (See section 3.2). In order to correct for this core environmental effect, a BP pin cell problem is defined for performing fine group transport calculations that properly correct the BP cross sections within the core diffusion calculation on-the-fly. As shown in Figure 2.1, the BP pin cell is defined as a cylindrical region containing the BP pin and its surrounding graphite. The fine group energy spectrum on the BP cell boundary is reconstructed using typical spectrum and the coarse group spectrum obtained from the whole core calculation. The BP pin cell local transport calculation with the reconstructed spectrum as boundary condition serves an imbedded module within the whole diffusion code to iteratively correct the BP absorption cross sections for improved results.

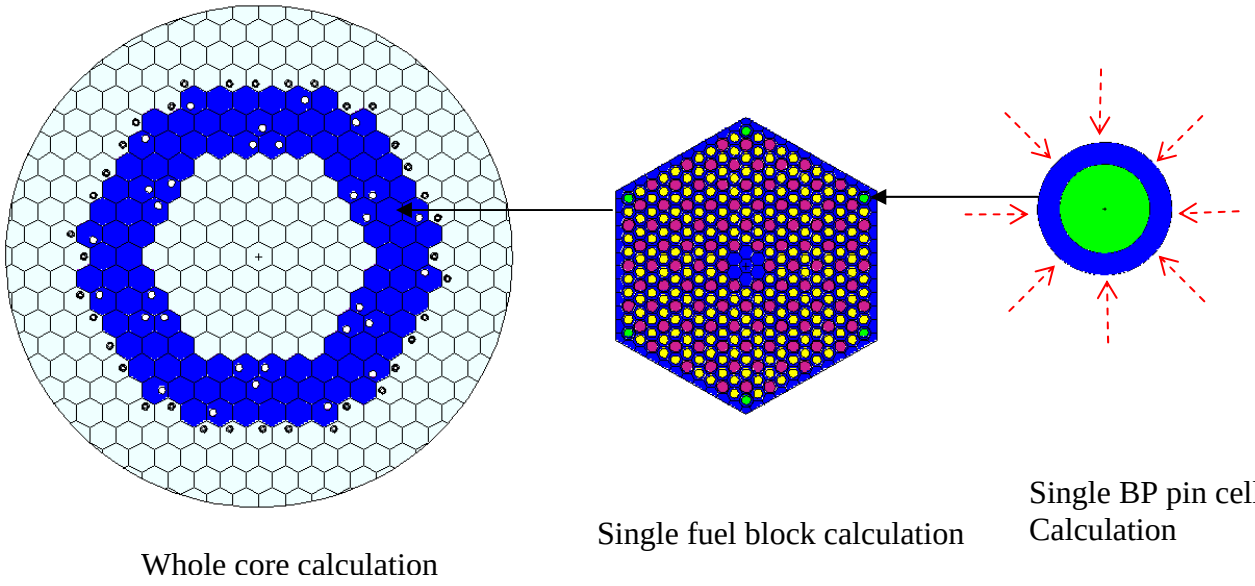

Figure 2.1. Whole core, single block and single BP cell model of prismatic HTR

2.2. Energy Reconstruction Methods

In order to reconstruct fine-group spectra from coarse-group spectra based on the "typical" spectra, two ESR methods are developed in this section: renormalization method and least square fitting method.

2.2.1 Renormalization method

The renormalization method reconstructs energy spectra by modulating the fine-group "typical" spectrum with the coarse-group spectra from whole core calculation.

Let Ψ_g and φ_h be the coarse and fine group fluxes (coarse group $g=1,2,\ldots G$; fine group $h=1,2,\ldots H$), respectively. These fluxes are normalized to one as defined below.

$$\hat{\Psi}_g = \frac{\Psi_g}{\sum_g \Psi_g} \quad ; \quad \hat{\varphi}_h = \frac{\varphi_h}{\sum_h \varphi_h} \tag{2.1}$$

Because the energy group widths vary up to several orders of magnitude, a change of variable is performed to use ln(*E*) as the independent variable of the energy spectrum . Taking the "typical" (TP) spectrum as an example, given "typical" fine group scalar flux $\hat{\varphi}_{h,TP}$, then the fine group spectrum is defined as

$$f_{TP}(w) = \frac{\hat{\varphi}_{h,TP}}{w_{h-1} - w_h}, w \in (w_h, w_{h-1}] \tag{2.2}$$

where, $w = \ln(E)$.

In the renormalization method, we simply renormalize the "typical" spectrum by the coarse group fluxes. That is, the fine group spectrum is obtained by renormalizing the "typical" spectrum so that it preserves the coarse group fluxes present in the whole core calculation.

$$f_{RN}(w) = \frac{\hat{\Psi}_g}{\int_g f_{TP}(w)dw} f_{TP}(w) \tag{2.3}$$

Hereafter, this spectrum will be referred to as "renormalized" spectrum.

2.2.2. Least Square Fitting Method

An alternative method is to obtain a continuous spectrum $f_{LS}(w)$ by minimizing its distance from the renormalized fine-group spectrum. Assume f_{LS} can be expanded by a set of B-spline bases (see Appendix A for the B-spline functions).

$$f_{LS}(w) = \sum_i c_i B_i(w) \tag{2.4}$$

In Eq. 2.4 , c_i and $B_i(w)$ are the *i*th expansion coefficient and the *i*th cubic B-spline basis. For the sake of clarity, the spectrum obtained via Eq. 2.4 is hereafter referred to as the "least square fitted" spectrum.

The normalization constraints and the desired minimization condition are satisfied by Eqs. 2.5 and 2.6, respectively.

$$\int_{w_{g-1}}^{w_g} f_{LS}(w)dw = \hat{\Psi}_g \text{ for } g=1,2,\ldots G \tag{2.5}$$

$$\text{Minimize } \delta = \int dw \left(f_{LS}(w) - f_{RN}(w) \right)^2 \tag{2.6}$$

Minimizing the functional given by Eq. 2.6 and conserving the coarse group fluxes in Eq. 2.5 requires the following Lagrangian to be stationary.

$$\Lambda = \int_{w_H}^{w_0} (\sum_i c_i B_i(w) - f_{RN}(w))^2 dw + \sum_g \lambda_g \left[\int_{w_g}^{w_{g-1}} \left(\sum_i c_i B_i(w) - \hat{\Psi}_g \right) dw \right] \tag{2.7}$$

Or equivalently,

$$\frac{\partial \Lambda}{\partial c_i} = \sum_j 2c_j \left\langle B_i, B_j \right\rangle - 2 \cdot \left\langle B_i, f_{RN} \right\rangle + \sum_g \lambda_g \int_{w_g}^{w_{g-1}} B_i(w)dw = 0 \tag{2.8}$$

$$\frac{\partial \Lambda}{\partial \lambda_g} = \sum_i c_i \int_{w_g}^{w_{g-1}} B_i(w)dw - \Psi_g = 0 \tag{2.9}$$

Once aforementioned linear system (Eqs. 2.8 and 2.9) is solved, the least square fitted spectrum $f_{LS}(w)$ can be reconstructed by substituting the coefficients c_i back to Eq. 2.4.

2.3 Response Method

The reconstructed spectra are used as boundary conditions of a single BP pin cell transport problem. BP absorptions cross sections are generated by solving this local transport problem. This local transport calculation is imbedded in the whole core diffusion calculation to correct BP absorption cross section on-the-fly.

The response function (RF) method of Forget, et al (2004) is extended to perform the local transport calculation and generate the BP absorption cross sections. As shown in this reference, the method is extremely fast while retaining transport accuracy. The method relies on absorption rate response and flux response due to a unit fine-group flux. Then, having these

responses one can immediately calculate the pin absorption cross sections in each coarse group by performing a simple linear superposition of response functions and reconstructed spectra, as follows.

The response absorption rate in the BP pin in coarse group *g* due a unit boundary flux in fine group *h'* is defined as

$$R_{a,g}^{h'} = \int_{V_{BP}} dv \int_{E_g}^{E_{g-1}} dE \int_{4\pi} d\hat{\Omega}\, \psi_{h'}\left(\vec{r}, \hat{\Omega}, E\right) \sigma_a\left(\vec{r}, E\right) \tag{2.10}$$

Similarly, the response flux in the BP pin in coarse group *g* due a unit boundary flux in fine group *h'* is defined as

$$F_g^{h'} = \int_{V_{BP}} dv \int_{E_g}^{E_{g-1}} dE \int_{4\pi} d\hat{\Omega}\, \psi_{h'}\left(\vec{r}, \hat{\Omega}, E\right) \tag{2.11}$$

The response function $\psi_{h'}\left(\vec{r}, \hat{\Omega}, E\right)$ is the solution to the following local fixed source problem in the pin cell.

$$\hat{\Omega} \cdot \nabla \psi_{h'}(\vec{r}, \hat{\Omega}, E) + \sigma_t(\vec{r}, E)\psi_{h'}(\vec{r}, \hat{\Omega}, E) + \int_0^{\infty} dE' \int_{4\pi} d\hat{\Omega}' \sigma_s(\vec{r}, E', \hat{\Omega}' \to E, \hat{\Omega})\psi_{h'}(\vec{r}, \hat{\Omega}, E) = 0 \tag{2.12}$$

The problem is solved by MCNP (X-5 Monte Carlo Team, 2003) with continuous energy cross section library, and with the isotropic flux boundary condition given below.

$$\psi_{h'}(\vec{r}, \hat{\Omega}, E) = \begin{cases} \dfrac{1}{2\pi}, & \text{for } \vec{r} \in \partial V,\ E \in (E_{h'}, E_{h'-1}] \text{ and } \hat{\Omega} \cdot \hat{n}^{-} > 0 \\ 0, & \text{otherwise} \end{cases} \tag{2.13}$$

It should be noted the boundary flux is assumed to be isotropic even though one can estimate a linearly anisotropic flux from the diffusion solution. This is a good assumption due the presence of graphite surrounding the pin. Its validity is verified in section 3.2.2. The response functions $R_{a,g}^{h'}$ and $F_g^{h'}$ are generated in advance as a pre-computed pin cell response library by MCNP since the pin cell configurations and the boundary condition given by Eq. 2.12 are known. Once the reconstructed spectrum $f(w)$ given by Eq. 2.3 or 2.4 is calculated by the ESR methods, the fine group fluxes are calculated by Eq. 2.14.

$$\hat{\varphi}_{h'} = \int_{w_{h'}}^{w_{h'-1}} f(w)dw \tag{2.14}$$

Then the absorption cross section for a burnable poison pin can be calculated as Eq. 2.15.

$$\bar{\sigma}_{a,g} = \frac{\sum_{h'} \hat{\varphi}_{h'} R_{a,g}^{h'}}{\sum_{h'} \hat{\varphi}_{h'} F_{g}^{h'}} \tag{2.15}$$

CHAPTER 3
HTR TEST PROBLEM AND SENSITIVITY ANALYSIS

In this chapter, the HTR test problem is described and sensitivity analysis is performed. The sensitivity analysis determines the number of fine groups and angular moment approximation for the energy spectra on the BP pin cell boundaries, and verifies the accuracy of single block calculated BP absorption cross sections. All MCNP calculations in this chapter are conducted with continuous energy cross section library at room temperature.

3.1 Problem Description

In this 2D prismatic HTR problem, the ESR methods were used to calculate the reconstructed energy spectrum on the boundary of each BP pin cell. With this spectrum, the absorption cross sections and absorption rates in each BP pin were calculated using the response method. In order to evaluate the combined ESR/response method developed in this study, the results from these calculations were then compared to the reference results generated by whole core MCNP calculations.

The test problem is obtained from the INEEL/EXT-04-02331 report (Sterberntz et al, 2002) and ANL-GenIV-075 report (Lee et al, 2006). In this problem, a fuel block consists of 204 fuel pins, 108 coolant channels, and 6 BP pins. The BP pin cell is defined as a 0.93 cm-radius cylindrical region containing the BP pin with some adjacent graphite as shown in Figure 3.1. There are 102 fuel blocks in the whole HTR core. The indexing of fuel blocks and BP pins are defined in Figure 3.1 and 3.2. The detailed description of geometry and material compositions can be found in the references INEEL/EXT-04-02331 and ANL-GenIV-075.

In order to generate the reference results, two 2D whole core prismatic HTR problems (controlled and uncontrolled) were calculated in MCNP with continuous energy cross section library. The controlled core (all control rods are fully inserted) is demonstrated in Figure 3.2, whereas for the uncontrolled core all control rods are removed. The reference results include coarse-group absorption cross sections for all BPs and fine-group fluxes on all BP cell

boundaries. For testing purposes, the coarse group fluxes, which should be acquired from whole core diffusion calculations, are also generated in the whole core MCNP calculation.

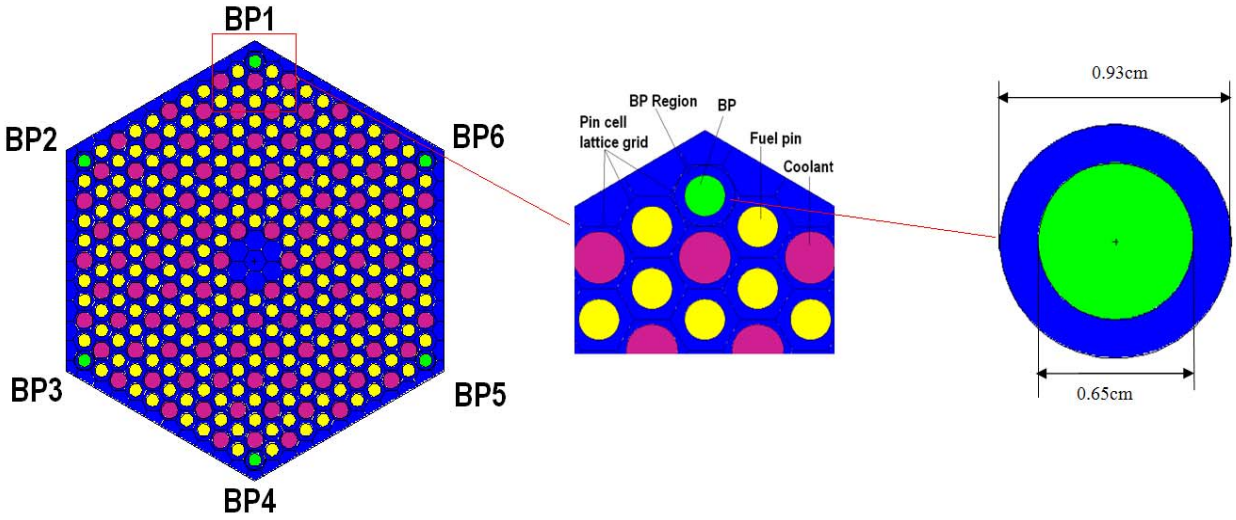

Figure 3.1. BP number indexing and detailed geometry in the fuel block

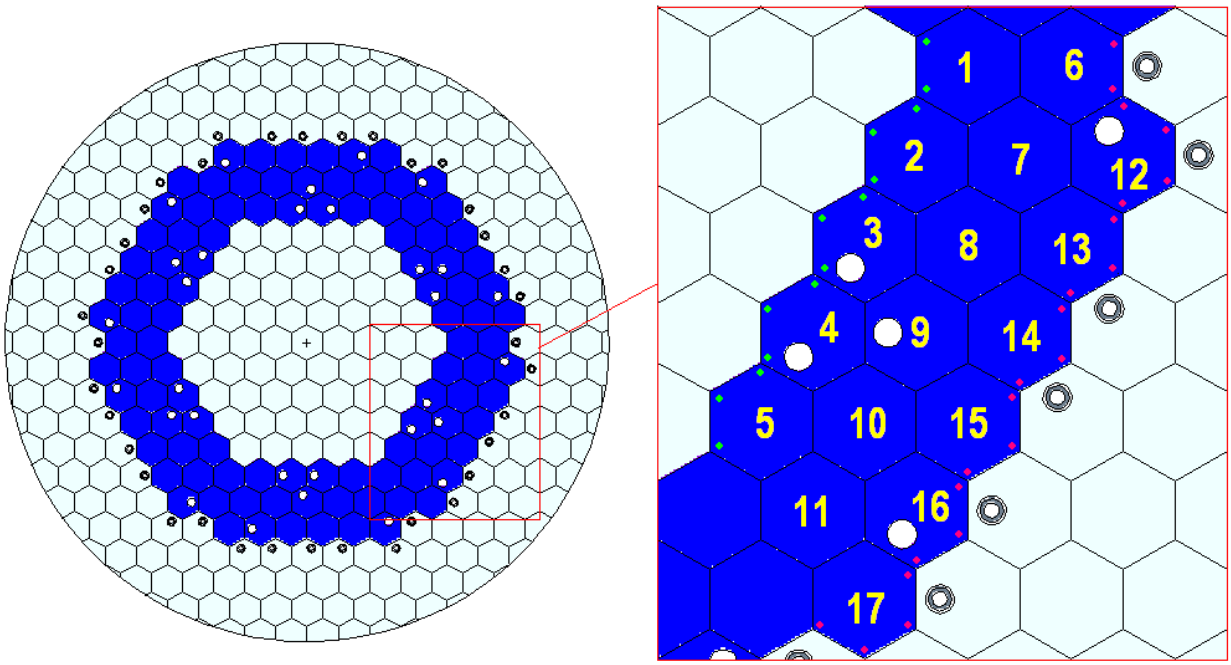

Figure 3.2. Whole core layout and fuel block indexing

In the 2D prismatic HTR, there are 17 different (unique) fuel blocks (see Figure 3.2) containing a total of 102 BP pins. These pins in controlled core are divided into 3 general categories:

Category 1: BP pins (14) neighboring reflector

Category 2: BP pins (66) neighboring fuel blocks

Category 3: BP pins (22) neighboring control rods

Only BPs in category 1(green) and category 3 (red) are illustrated in Figure 3.2.

The average fine group spectrum for each category calculated in the controlled configuration is shown in Figure 3.3, and they are used as the "typical" spectrum for each category, respectively. It can be seen that the three categories are distinctly different. It was also found that the "typical" spectrum categories for the uncontrolled configuration were very similar to the controlled configuration. That is, using the controlled "typical" spectra in the ESR methods for the uncontrolled case led to similar results as the reference solutions of the uncontrolled case (see section 4.1.2).

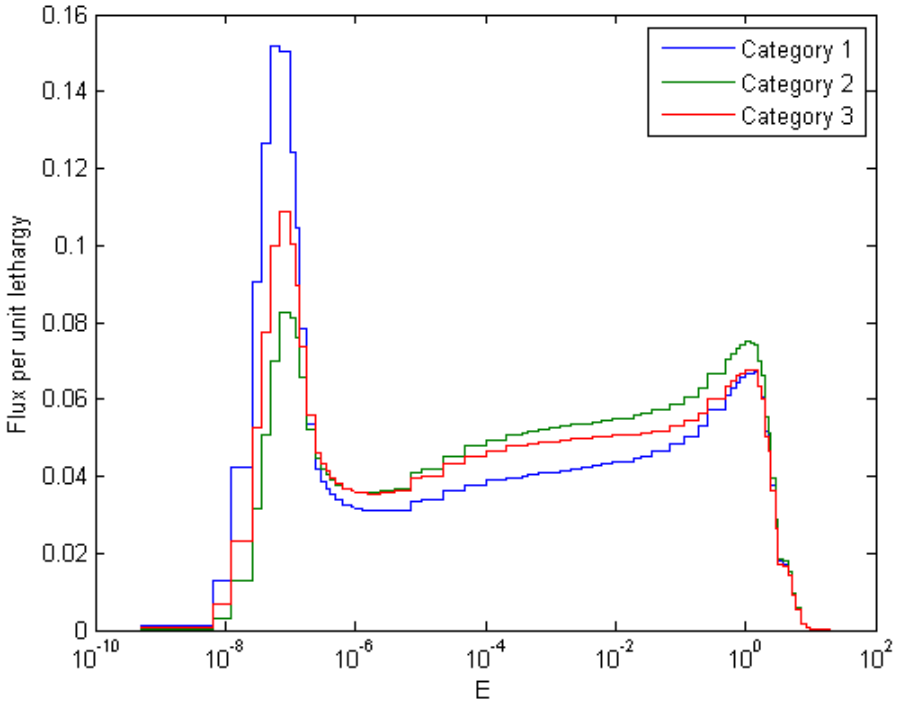

Figure 3.3. "Typical" spectra for three categories in the controlled core

3.2 Sensitivity Analysis

A number of sensitivity studies are performed to investigate: (1) how fine the energy groups can sufficiently represent the actual energy distribution on the BP pin cell boundaries; (2) which order in the angular expansion is required for the pin cell boundary condition; and (3) what is the accuracy of single block calculated BP absorption cross sections. In order to exclude the errors associated with the incoming energy spectra, the reference results (spectra) obtained from MCNP calculations rather than reconstructed by the ESR methods are used in the sensitivity analyses.

3.2.1 Energy Group Structure Effect

The 7-group structure in the ANL-GenIV-075 report is used as the coarse group structure in this study. 30 and 71group structures are selected by refining the 7 group structure arbitrarily, to determine how fine the group structure needs to be for accurate BP absorption cross section calculations. The energy boundaries are given in Table B.1 in Appendix B.

A single fuel block MCNP calculation with continuous energy cross sections and specular reflection boundary was conducted as the reference problem for determining the fine group structure. In this calculation, 30-group and 71-group energy spectra on the BP pin cell boundary were tallied. The 7-group absorption cross sections $\sigma_{a,g}^{ref}$ and BP pin group fluxes ϕ_g were also tallied. Then, two sets of BP coarse group absorption cross sections are calculated using the fine group spectra from the single block calculation as boundary conditions in single BP cell continuous energy MCNP calculations. The total absorption rates are then calculated by as given below.

$$R_a = \sum_g \sigma_{a,g}\phi_g \tag{3.1}$$

Comparing the single BP cell calculation results with reference results in Table 3.1, it was found that the 30-group energy spectrum is not sufficient to reproduce the reference 7-group

absorption cross sections (300% error in the fast group cross sections, and 6% error in the total absorption rate). In contrast, the 71-group energy spectrum reasonably reproduced the reference absorption cross sections. Although the cross section errors were up to 1% for group 1 and 3, they contribute little to the total absorption rates. The error in the total absorption rate in the 71-group results was only 0.44%.Therefore, it can be concluded that 71- group structure is sufficient for the validation of the methods.

Table 3.1. Absorption cross section errors introduced by different group numbers of the BP pin cell boundary conditions (single block energy spectra)

	Group upper boundary	Reference	30G errors	71G errors
G7 XS*	1.0000E-07	4.47102E-01	8.87%	-0.29%
G6 XS	5.0000E-07	2.22406E-01	-0.53%	-0.54%
G5 XS	1.0970E-06	1.13605E-01	-0.23%	-0.22%
G4 XS	4.0000E-06	6.80086E-02	0.44%	-0.57%
G3 XS	9.1180E-03	1.10662E-02	-45.52%	-1.21%
G2 XS	5.0000E-01	4.18460E-04	-2.38%	-0.80%
G1 XS	2.0000E+01	8.49760E-05	340.63%	0.97%
Ab. Rate**		1.59259E-01	5.98%	-0.44%

* G7 XS: Group7 absorption cross section
** Ab. Rate: absorption rates
*** Statistical uncertainties are all less than 0.06%

3.2.2 Angular Approximation Effect

In this section, the effect of angular flux approximation on the BP cell boundary is analyzed. First, a single block MCNP calculation with specular reflection boundary was used as the reference problem, in which, fine-group energy spectra for both scalar fluxes and net currents on the BP cell boundary were tallied. In the BP pin cell calculations with isotropic (scalar flux only) and linearly anisotropic (scalar flux and net current) boundary conditions, two sets of coarse group absorption cross sections were generated for the BP pin. A comparison of these results to those from the reference single block MCNP calculation is shown in Table 3.2. It is

seen that for most groups, the errors are less than 1%. As indicated by the comparison of the results in the last two columns of Table 3.2, no statistically significant improvement is seen by using the linearly anisotropic boundary condition.

Table 3.2. Absorption cross section errors introduced by different angular approximations of the BP pin cell boundary conditions (single block energy spectra)

	Group upper boundary	Reference	Linear anisotropic errors	Isotropic errors
G7 XS*	1.0000E-07	4.47102E-01	-0.04%	-0.29%
G6 XS	5.0000E-07	2.22406E-01	-0.45%	-0.54%
G5 XS	1.0970E-06	1.13605E-01	-0.21%	-0.22%
G4 XS	4.0000E-06	6.80086E-02	-0.55%	-0.57%
G3 XS	9.1180E-03	1.10662E-02	-1.14%	-1.21%
G2 XS	5.0000E-01	4.18460E-04	-0.83%	-0.80%
G1 XS	2.0000E+01	8.49760E-05	1.24%	0.97%
Ab. Rate**		1.59259E-01	-0.27%	-0.44%

* G7 XS: Group7 absorption cross section
** Ab. Rate: absorption rates
*** Statistical uncertainties are all less than 0.06%

Second, same comparisons were made in the controlled configuration of whole core problem. The corresponding errors for all the 102 BP pins in the whole core are summarized by collective errors defined in Appendix C, as shown in Table 3.3.

Table 3.3. Collective errors in absorption cross sections introduced by different angular approximations of the BP pin cell boundary conditions (reference energy spectra for all the102 BP pins)

	Errors in single BP cell calculation with linear anisotropic spectra			
	AVG	MAX	RMS	MRE
G7 XS	0.13%	0.34%	0.15%	0.13%
G6 XS	0.48%	0.65%	0.48%	0.48%
G5 XS	0.21%	0.30%	0.21%	0.21%
G4 XS	0.55%	0.67%	0.55%	0.55%
G3 XS	1.14%	1.39%	1.14%	1.14%
G2 XS	0.83%	1.04%	0.83%	0.83%
G1 XS	1.47%	6.92%	1.69%	1.46%
Ab. rate	0.30%	0.40%	0.30%	0.31%

Table 3.3. (continued) Collective Errors in absorption cross sections introduced by different angular approximations of the BP pin cell boundary conditions (reference energy spectra for all the102 BP pins)

	Errors in single BP cell calculation with isotropic spectra			
	AVG	MAX	RMS	MRE
G7 XS	0.42%	0.72%	0.43%	0.42%
G6 XS	0.58%	0.75%	0.58%	0.58%
G5 XS	0.22%	0.31%	0.23%	0.22%
G4 XS	0.57%	0.70%	0.58%	0.57%
G3 XS	1.21%	1.49%	1.21%	1.21%
G2 XS	0.80%	1.01%	0.80%	0.80%
G1 XS	1.23%	6.58%	1.47%	1.22%
Ab. rate	0.51%	0.71%	0.51%	0.53%
	Uncertainties of the reference absorption cross sections and absorption rates			
	AVG	MAX	RMS	MRE
G7 XS	0.23%	0.33%	0.24%	0.23%
G6 XS	0.26%	0.41%	0.26%	0.26%
G5 XS	0.44%	0.77%	0.45%	0.44%
G4 XS	0.36%	0.64%	0.37%	0.36%
G3 XS	0.17%	0.31%	0.18%	0.17%
G2 XS	0.19%	0.35%	0.20%	0.19%
G1 XS	0.75%	1.37%	0.77%	0.75%
Ab. rate	0.11%	0.16%	0.11%	0.10%

* G7 XS: Group7 absorption cross section
** Ab. Rate: absorption rates

It can be seen that the mean relative errors (MRE) are less than 1% except in two fast groups (Group 1 and 3), which contribute little to the total absorption rates.

Based on the analysis presented in this section it can be concluded that the single BP cell calculation with the reference fine-group (71) boundary condition can reproduce the BP pin absorption cross sections and absorption rates accurately. It is also concluded that the angular effect on the boundary condition is not significant statistically and therefore one can use the isotropic boundary condition for the BP pin cell calculations.

It is worth noting that the reasons for the small errors observed in this analysis are likely due to the choice of the group structure (energy boundaries) and the fact that the structure may not be fine enough. The angular effects are not as pronounced and can be neglected.

3.2.3 Accuracy of Single Block Calculated BP Pin Cross Sections

Single bundle calculation with specular reflection boundary is commonly used to generate multi-group cross sections. In this section, it is shown that this practice leads to large errors in the BP absorption cross sections. This is demonstrated for the controlled configuration of the 2D prismatic HTR core. BP absorption cross sections and absorption rates generated in single block calculation (specular reflection boundary) are compared to those calculated directly from a whole core reference solution, and the collective errors (see Appendix C) are presented in Table 3.4. In both cases continuous energy MCNP is used to perform the calculations. It is observed from Table 3.4 that the cross section errors in the BP pins neighboring a reflector are large (as high as almost 8% MRE in the thermal group). The errors in those neighboring fuel blocks are negligible as expected. The errors in those neighboring control rods are not negligible but smaller than those near a reflector block.

Based on the results presented in this section, it can be concluded that the absorption cross sections in the BP pins that are not neighboring a fuel block must be corrected for the single block spectral effects by using the methods developed in this thesis.

Table 3.4. Collective errors in BP absorption cross sections calculated by single block model

Category 1				
	AVG	MAX	RMS	MRE
G7 XS	7.72%	10.02%	7.86%	7.74%
G6 XS	4.10%	6.16%	4.29%	4.11%
G5 XS	0.05%	0.13%	0.06%	0.05%
G4 XS	0.09%	0.24%	0.12%	0.09%
G3 XS	1.40%	2.77%	1.65%	1.41%
G2 XS	2.02%	2.59%	2.05%	2.02%
G1 XS	2.50%	4.46%	2.77%	2.51%
Ab. rate	6.43%	8.96%	6.62%	6.73%

Table 3.4.(continued) Collective errors in BP absorption cross sections calculated by single block model

Category 2				
	AVG	MAX	RMS	MRE
G7 XS	0.53%	2.35%	0.77%	0.53%
G6 XS	0.21%	0.85%	0.28%	0.21%
G5 XS	0.03%	0.09%	0.04%	0.03%
G4 XS	0.07%	0.16%	0.08%	0.07%
G3 XS	2.08%	3.64%	2.19%	2.08%
G2 XS	0.53%	1.12%	0.58%	0.53%
G1 XS	0.45%	1.24%	0.55%	0.45%
Ab. rate	0.25%	1.46%	0.41%	0.30%
Category 3				
	AVG	MAX	RMS	MRE
G7 XS	4.35%	8.07%	4.88%	4.41%
G6 XS	1.68%	4.02%	2.04%	1.69%
G5 XS	0.04%	0.09%	0.05%	0.04%
G4 XS	0.08%	0.21%	0.10%	0.08%
G3 XS	1.36%	3.40%	1.61%	1.36%
G2 XS	0.35%	1.05%	0.48%	0.35%
G1 XS	1.29%	3.79%	1.60%	1.30%
Ab. rate	3.21%	6.77%	3.77%	3.28%

* G7 XS: Group7 absorption cross section
** Ab. Rate: absorption rates

CHAPTER 4
RESULTS

In the prismatic HTR test problem, the ESR methods reconstruct fine group spectra on the BP cell boundaries, and they are used as boundary conditions in local BP cell problems, which are solved by response method. Figure 4.1 shows the flowchart of the test process. In this chapter, all reference calculations and response function generations are conducted by MCNP with continuous energy cross section library at room temperature. In all the tables of this Chapter, the collective errors are referred to the definitions in Appendix C, and the following abbreviations are used:

SB: Single block energy spectrum

RN: Renormalized energy spectrum

LS: Least squared fitted energy spectrum

Ref: Reference energy spectrum

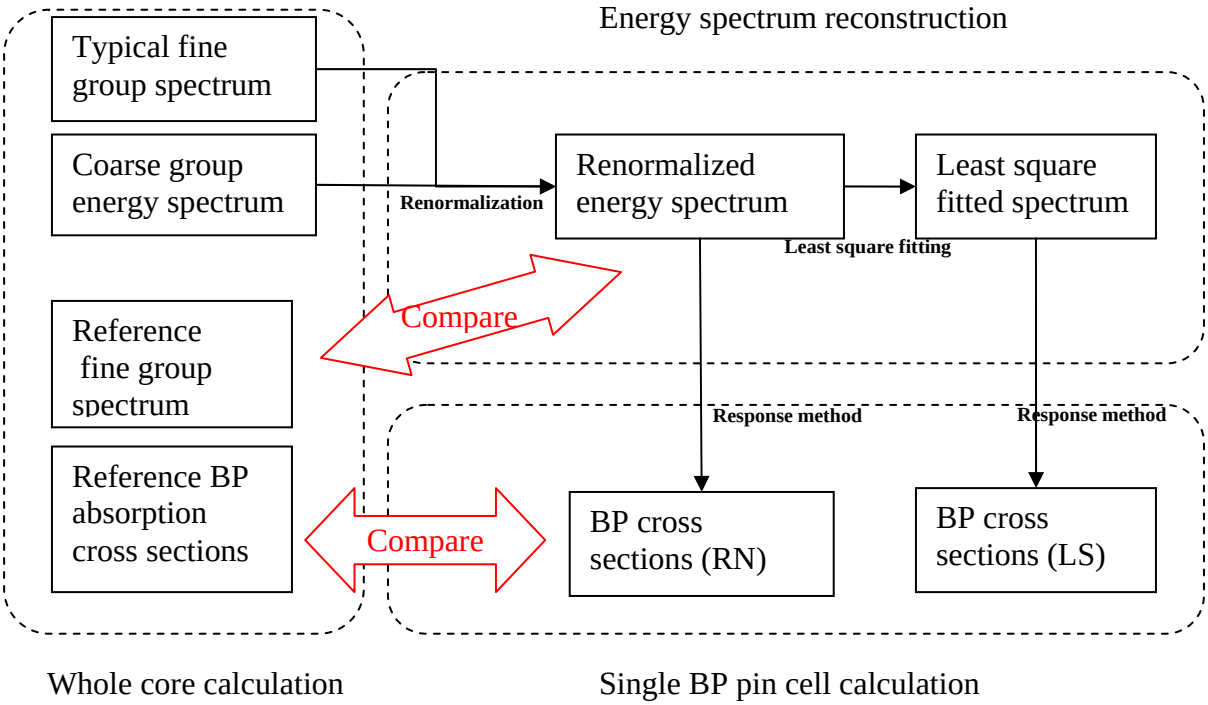

Figure 4.1. Flowchart of the test process

4.1 Reconstructed Energy Spectrum Results

The ESR methods described in the previous sections were tested in two different configurations of the prismatic HTR test problem, namely, the controlled and uncontrolled configurations. The reconstructed energy spectra calculated using both the renormalization and the least square fitting method as well as the energy spectra directly found from the single block calculation were compared to the reference spectra. Note that the least square fitted spectra were put into the multi-group format in this comparison. The error as compared to the reference spectrum over all groups is defined in Eq. 4.1, where, $\hat{\varphi}_{x,h}$ is the corresponding flux (Eq. 4.2) in each fine group *h* calculated using the three different methods discussed in this report (i.e., renormalization, least square fitting and single block methods).

$$e_x = \frac{\sum_h \left| \hat{\varphi}_{x,h} - \hat{\varphi}_{ref,h} \right|}{\sum_h \left| \hat{\varphi}_{ref,h} \right|} \tag{4.1}$$

$$\hat{\varphi}_{x,h} = \int_{w_h}^{w_{h-1}} f_x(w) dw \tag{4.2}$$

4.1.1 Energy Spectrum Results for Controlled Core

Figure 4.2 is a comparison of the estimated spectra (renormalized, least square fitted and single block) to the reference spectrum for BP pin # 2 in fuel block 4 (indexing can be found in Figures 3.1 and 3.2). As in Figure 4.2, both of the new methods generate good energy spectra whereas the single block spectrum is relatively poor as compared to the reference spectrum.

In Table 4.1, the errors in reconstructed spectra are compared to those in single block energy spectra. The reconstructed energy spectra are in good agreement with the reference spectra (all less than 5% error), while the single block spectrum has large discrepancy with the reference spectra (as large as 50% error). Clearly, these large errors are the cause of the inaccuracy in BP absorption cross sections in Table 3.4.

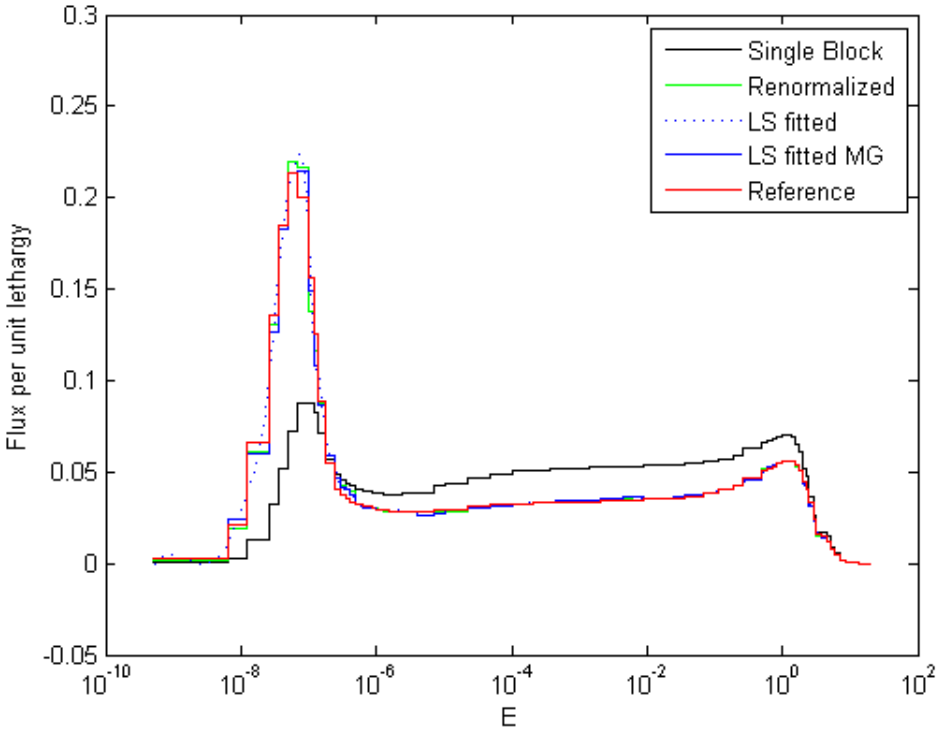

Figure 4.2. Energy spectrum reconstruction for BP pin #2 in fuel block 4 of the controlled core

Table 4.1. Errors in single block spectra and reconstructed spectra in the controlled core

	SB vs Ref					
	Pin 1	Pin 2	Pin 3	Pin 4	Pin 5	Pin 6
Block 1	5.76%	17.80%	17.80%	5.75%	4.45%	4.54%
Block 2	18.93%	46.93%	20.63%	6.78%	5.23%	6.03%
Block 3	20.75%	47.22%	21.17%	6.73%	4.78%	6.74%
Block 4	21.29%	47.50%	21.20%	6.90%	4.29%	6.56%
Block 5	21.38%	47.24%	19.05%	6.14%	5.33%	6.76%
Block 6	3.83%	4.32%	4.24%	3.07%	***2.91%***	***3.55%***
Block 7	4.33%	5.35%	4.92%	4.01%	3.79%	3.24%
Block 8	4.93%	5.96%	4.59%	3.69%	3.62%	3.87%
Block 9	4.44%	5.01%	3.58%	3.47%	3.51%	3.66%
Block 10	3.99%	5.73%	5.02%	3.76%	3.72%	3.68%
Block 11	4.96%	5.46%	4.33%	3.81%	3.17%	3.79%
Block 12	***3.63%***	2.74%	3.76%	***12.31%***	***26.77%***	***19.02%***
Block 13	3.84%	4.02%	3.70%	***3.86%***	***22.01%***	***11.93%***
Block 14	3.79%	3.70%	3.68%	***3.67%***	***14.75%***	***3.65%***
Block 15	3.69%	3.65%	3.71%	***4.58%***	***22.96%***	***4.39%***
Block 16	3.59%	3.59%	2.58%	***4.53%***	***15.28%***	***3.77%***
Block 17	2.94%	3.85%	***3.91%***	***30.46%***	***24.34%***	***3.96%***

Table 4.1(continued) Errors in single block spectra and reconstructed spectra in the controlled core

	RN vs Ref					
	Pin 1	Pin 2	Pin 3	Pin 4	Pin 5	Pin
Block 1	0.74%	1.76%	1.81%	0.71%	0.40%	0.34%
Block 2	1.49%	3.42%	1.42%	1.13%	0.34%	0.84%
Block 3	1.40%	3.57%	1.19%	1.39%	0.37%	1.19%
Block 4	1.18%	3.62%	1.29%	1.41%	0.38%	1.28%
Block 5	1.22%	3.45%	1.62%	0.87%	0.42%	1.28%
Block 6	0.62%	0.47%	0.52%	0.71%	***1.84%***	***1.88%***
Block 7	0.55%	0.45%	0.39%	0.60%	0.39%	0.54%
Block 8	0.43%	0.70%	0.29%	0.69%	0.63%	0.77%
Block 9	0.23%	0.79%	0.33%	0.65%	0.58%	0.67%
Block 10	0.28%	0.86%	0.41%	0.66%	0.53%	0.69%
Block 11	0.43%	0.46%	0.47%	0.53%	0.59%	0.70%
Block 12	***1.53%***	0.54%	0.51%	***1.16%***	***3.76%***	***2.20%***
Block 13	0.44%	0.65%	0.63%	***1.68%***	***2.54%***	***1.11%***
Block 14	0.63%	0.68%	0.54%	***1.57%***	***1.48%***	***1.39%***
Block 15	0.53%	0.65%	0.56%	***1.29%***	***3.12%***	***1.28%***
Block 16	0.60%	0.80%	0.59%	***1.33%***	***1.61%***	***1.60%***
Block 17	0.57%	0.51%	***1.36%***	***4.93%***	***3.36%***	***1.34%***
	LS vs Ref					
	Pin 1	Pin 2	Pin 3	Pin 4	Pin 5	Pin 6
Block 1	0.91%	1.88%	1.92%	0.93%	0.66%	0.63%
Block 2	1.68%	3.25%	1.64%	1.28%	0.71%	1.02%
Block 3	1.69%	3.28%	1.51%	1.43%	0.69%	1.31%
Block 4	1.46%	3.39%	1.57%	1.49%	0.69%	1.35%
Block 5	1.49%	3.22%	1.78%	1.03%	0.75%	1.35%
Block 6	0.82%	0.71%	0.73%	0.88%	***1.78%***	***1.86%***
Block 7	0.81%	0.81%	0.67%	0.79%	0.67%	0.75%
Block 8	0.72%	0.93%	0.67%	0.87%	0.77%	0.93%
Block 9	0.61%	0.95%	0.67%	0.80%	0.72%	0.80%
Block 10	0.60%	1.03%	0.68%	0.84%	0.76%	0.82%
Block 11	0.67%	0.78%	0.73%	0.73%	0.76%	0.85%
Block 12	***1.55%***	0.81%	0.72%	***1.44%***	***3.31%***	***2.08%***
Block 13	0.78%	0.76%	0.76%	***1.75%***	***2.35%***	***1.45%***
Block 14	0.76%	0.79%	0.77%	***1.61%***	***1.55%***	***1.42%***
Block 15	0.69%	0.79%	0.71%	***1.36%***	***2.96%***	***1.33%***
Block 16	0.78%	0.91%	0.85%	***1.43%***	***1.63%***	***1.62%***
Block 17	0.81%	0.74%	***1.44%***	***4.34%***	***2.98%***	***1.39%***

* Shaded cell : Category 1; ***Bold Italic font:*** Category 3

** SB: single block spectra; Ref: reference energy spectra;
RN: renormalized spectra; LS: least square fitted spectra

Table 4.2 summarizes the collective percent errors in the single block and reconstructed energy spectra for the three BP categories. The ESR methods reduced the single block errors significantly, e.g., the MRE is reduced from 28% to 2% for category 1 and from 10% to 2% as in category 3. It is noted that both the renormalized and the least square fitted spectra have similar accuracy. Therefore, it is recommended to use the simple renormalization method to obtain the fine group spectra unless continuous energy spectra are needed in which case one would use the least square fitting method.

Table 4.2. Collective errors in single block spectra and reconstructed spectra in the controlled core

		AVG	MAX	RMS	MRE
Category 1	SB	27.78%	47.50%	30.40%	27.60%
	RN	2.03%	3.62%	2.24%	2.02%
	LS	2.13%	3.39%	2.25%	2.12%
Category 2	SB	4.43%	6.90%	4.56%	4.60%
	RN	0.62%	1.41%	0.67%	0.64%
	LS	0.83%	1.49%	0.86%	0.85%
Category 3	SB	11.19%	30.46%	14.36%	9.91%
	RN	1.97%	4.93%	2.19%	1.86%
	LS	1.94%	4.34%	2.08%	1.85%

* SB: single block spectra; RN: renormalized spectra; LS: least square fitted spectra

4.1.2 Energy Spectrum for Uncontrolled Core

In this section, it is demonstrated that a “typical” spectra derived from given controlled core configuration can be used in problems of different configurations. To show the robustness of the method, the “typical” spectra from the previous section (i.e., the controlled configuration) is used in the uncontrolled core. Note that in this uncontrolled case, there are two category 1 situations: “category 1 inner” where the BP pins are neighboring inner reflector blocks and “category 1 outer” where the BP pins are neighboring the outer reflector blocks. The “category 1 outer” BPs in uncontrolled core are at the identical locations of the “category 3” BPs in controlled core.

The single block and the reconstructed spectra errors are shown in Table 4.3. The single block spectra have significant errors (up to 50%) as compared to the reconstructed spectra where the errors are less than 3.5%.

Table 4.3. Errors in single block spectra and reconstructed spectra in the uncontrolled core

	SB vs Ref					
	Pin 1	Pin 2	Pin 3	Pin 4	Pin 5	Pin 6
Block 1	3.87%	18.65%	18.43%	3.98%	2.72%	2.76%
Block 2	19.63%	48.43%	21.44%	5.16%	3.12%	4.25%
Block 3	21.44%	48.91%	22.30%	5.50%	2.85%	5.04%
Block 4	22.28%	49.18%	22.31%	5.67%	2.73%	5.25%
Block 5	22.25%	48.57%	19.70%	4.32%	3.25%	5.41%
Block 6	4.07%	2.82%	2.73%	4.21%	***17.65%***	***16.85%***
Block 7	2.82%	3.43%	2.84%	2.75%	4.11%	3.63%
Block 8	2.84%	4.11%	2.49%	2.55%	3.62%	2.76%
Block 9	2.41%	3.73%	1.94%	2.36%	3.53%	2.64%
Block 10	2.23%	4.35%	2.87%	2.60%	3.66%	2.41%
Block 11	2.92%	3.41%	2.82%	3.69%	4.03%	2.63%
Block 12	***18.63%***	4.91%	5.18%	***19.72%***	***48.70%***	***47.85%***
Block 13	4.88%	2.96%	4.40%	***20.15%***	***44.09%***	***19.47%***
Block 14	4.38%	2.88%	4.40%	***20.24%***	***44.05%***	***19.69%***
Block 15	4.30%	2.80%	4.45%	***19.82%***	***44.01%***	***19.89%***
Block 16	4.42%	2.85%	5.03%	***20.32%***	***44.29%***	***20.30%***
Block 17	5.36%	4.53%	***17.63%***	***46.77%***	***47.28%***	***20.88%***
	RN vs Ref					
	Pin 1	Pin 2	Pin 3	Pin 4	Pin 5	Pin 6
Block 1	0.82%	2.20%	2.24%	0.76%	0.88%	0.81%
Block 2	1.95%	3.49%	1.55%	0.98%	0.82%	0.81%
Block 3	1.61%	3.46%	1.57%	1.28%	0.81%	1.01%
Block 4	1.50%	3.44%	1.62%	1.28%	0.86%	1.06%
Block 5	1.45%	3.37%	1.89%	0.80%	0.72%	1.10%
Block 6	0.78%	0.83%	0.77%	0.97%	***2.48%***	***2.39%***
Block 7	0.89%	0.69%	0.86%	0.88%	0.75%	0.80%
Block 8	0.91%	0.74%	0.87%	0.93%	0.68%	0.81%
Block 9	0.90%	0.98%	0.92%	0.85%	0.79%	0.86%
Block 10	0.99%	0.80%	0.81%	0.89%	0.69%	0.87%
Block 11	0.83%	0.70%	0.86%	0.71%	0.81%	0.84%
Block 12	***2.34%***	1.10%	0.90%	***1.77%***	***3.51%***	***3.46%***
Block 13	1.02%	0.80%	0.79%	***1.66%***	***2.91%***	***1.83%***
Block 14	0.83%	0.84%	0.83%	***1.67%***	***2.88%***	***1.76%***
Block 15	0.79%	0.81%	0.79%	***1.81%***	***2.83%***	***1.72%***
Block 16	0.93%	0.76%	1.12%	***1.82%***	***2.97%***	***1.69%***
Block 17	1.02%	0.83%	***2.15%***	***3.09%***	***3.18%***	***1.67%***

Table 4.3.(continued) Errors in single block spectra and reconstructed spectra in the uncontrolled core

	LS vs Ref					
	Pin 1	Pin 2	Pin 3	Pin 4	Pin 5	Pin 6
Block 1	0.46%	2.16%	2.20%	0.43%	0.62%	0.56%
Block 2	1.82%	3.65%	1.26%	0.73%	0.47%	0.50%
Block 3	1.32%	3.70%	1.26%	1.19%	0.53%	0.82%
Block 4	1.19%	3.65%	1.34%	1.17%	0.67%	1.00%
Block 5	1.17%	3.55%	1.75%	0.52%	0.35%	0.89%
Block 6	0.47%	0.59%	0.58%	0.75%	***2.43%***	***2.34%***
Block 7	0.66%	0.34%	0.66%	0.71%	0.43%	0.58%
Block 8	0.65%	0.43%	0.64%	0.69%	0.35%	0.59%
Block 9	0.55%	0.86%	0.70%	0.65%	0.43%	0.68%
Block 10	0.72%	0.59%	0.57%	0.57%	0.38%	0.63%
Block 11	0.59%	0.38%	0.62%	0.33%	0.54%	0.61%
Block 12	***2.32%***	0.94%	0.71%	***1.56%***	***3.72%***	***3.55%***
Block 13	0.76%	0.50%	0.53%	***1.44%***	***2.88%***	***1.67%***
Block 14	0.56%	0.54%	0.57%	***1.41%***	***2.84%***	***1.58%***
Block 15	0.53%	0.49%	0.53%	***1.62%***	***2.74%***	***1.54%***
Block 16	0.62%	0.49%	0.96%	***1.61%***	***2.98%***	***1.45%***
Block 17	0.83%	0.60%	***2.07%***	***3.14%***	***3.34%***	***1.41%***

* Shaded cell : Category 1 inner; ***Bold Italic font:*** Category 1 outer
** SB: single block spectra; Ref: reference energy spectra;
RN: renormalized spectra; LS: least square fitted spectra

The collective errors in the reconstructed spectra are presented in Table 4.4. Like in the controlled case, both of the ESR methods reduce the MRE from 28% to 2% for both category 1 cases.

Table 4.4. Collective errors in single block spectra and reconstructed spectra in the uncontrolled core

		AVG	MAX	RMS	MRE
Category 1 inner	SB	28.82%	49.18%	31.49%	28.50%
	RN	2.14%	3.70%	2.37%	2.13%
	LS	2.24%	3.49%	2.38%	2.23%
Category 2	SB	3.63%	5.67%	3.76%	3.62%
	RN	0.61%	1.19%	0.64%	0.61%
	LS	0.87%	1.28%	0.88%	0.87%
Category 1 outer	SB	29.01%	48.70%	31.72%	28.30%
	RN	2.26%	3.72%	2.38%	2.22%
	LS	2.35%	3.51%	2.43%	2.31%

* SB: single block spectra; RN: renormalized spectra; LS: least square fitted spectra

4.2. Absorption Cross Section Results

As seen in the previous section, the reconstructed energy spectra are significantly better than the single block spectra. In this section, we evaluate how well the new ESR methods improve BP pin absorption cross sections as compared to the commonly used single block results.

Using energy spectra as boundary conditions in the BP pin cell model, coarse-group BP absorption cross sections were generated by the response transport method. Table 4.5 shows the comparison of errors in BP absorption cross sections generated by different methods for a selected BP pin (BP #2 in fuel block 4). Using the reference MCNP whole core coarse group fluxes and the different coarse group cross sections into Eq. 3.1, the total absorption rates are calculated for different energy spectra. The errors in absorption rates are presented in Table 4.6 for fuel block 4. The MCNP whole core coarse group fluxes are used in the absorption rate calculation (as Eq. 3.1) because the use of single block fluxes would be inconsistent with the corresponding reference and ESR methods values otherwise.

As a category 1 BP pin (BP #2 in fuel block 4) shown in Table 4.5, although the error in the ESR methods may be slightly higher than the single block case for the fast groups 1 and 3, the total absorption rate is significantly better than the single block result (9% versus 1-3%). The absorption rate error represents the collective effect of all group cross section errors, so hereafter only the absorption rate errors are analyzed. The reference absorption cross sections and errors for different methods are presented in Appendix D. As seen from Table 4.6, for category 1 BP pins (pins 1-3), the absorption rate errors are reduced from 5-9% to less than 3%. For category 2 (see pins 4-6), the single block results seem to be accurate enough. However, the least square fitting method still improves the accuracy.

Table 4.5. Absorption cross section errors for BP pin # 2 in fuel block 4

		Controlled core			Uncontrolled core		
	Pin 2	SB	RN	LS	SB	RN	LS
G7 XS	4.97E-01	-10.02%	-2.67%	-1.15%	-9.99%	-2.75%	-1.12%
G6 XS	2.37E-01	-6.16%	-2.55%	-2.11%	-6.20%	-2.60%	-2.15%
G5 XS	1.14E-01	-0.05%	-0.22%	-0.16%	-0.06%	-0.20%	-0.16%
G4 XS	6.82E-02	-0.24%	-0.64%	-0.57%	-0.26%	-0.66%	-0.57%
G3 XS	1.14E-02	-2.65%	-3.93%	-3.71%	-3.08%	-3.59%	-4.08%
G2 XS	4.08E-04	2.58%	-0.29%	-0.30%	2.26%	-0.29%	-0.57%
G1 XS	8.82E-05	-3.70%	-0.36%	5.44%	-4.44%	-1.52%	4.44%
Ab. rate	6.46E-04	-8.96%	-2.60%	-1.32%	-8.95%	-2.66%	-1.31%

* SB: single block calculation; RN: renormalized spectra; LS: least square fitted spectra

Table 4.6. Absorption rate errors for fuel block 4

		Pin 1	Pin 2	Pin 3	Pin 4	Pin 5	Pin 6
Controlled core	SB	-5.68%	-8.96%	-5.75%	-1.34%	-0.47%	-1.20%
	RN	0.30%	-2.60%	0.22%	-1.51%	-0.71%	-1.39%
	LS	1.00%	-1.32%	0.93%	-0.75%	-0.16%	-0.66%
Uncontrolled core	SB	-5.66%	-8.95%	-5.66%	-1.38%	-0.52%	-1.24%
	RN	0.27%	-2.66%	0.27%	-1.32%	-0.52%	-1.18%
	LS	1.04%	-1.31%	1.03%	-0.79%	-0.18%	-0.67%

* SB: single block calculation; RN: renormalized spectra; LS: least square fitted spectra

Table 4.7 presents the collective errors in absorption rates for all BP pins in the whole core. The ESR methods reduce the MRE of absorption rates from 6.7% to less than 1.5% for category 1 BP pins, and from 3.3% to less than 1.5% for category 3 BP pins. The collective errors for absorption cross sections in each coarse group are presented in Appendix D.

Table 4.7. Collective errors in absorption rates for all BP pins in the whole core

	Controlled core								
	Category 1			Category 2			Category 3		
	SB	RN	LS	SB	RN	LS	SB	RN	LS
AVG	6.43%	1.07%	1.18%	0.25%	0.43%	0.20%	3.21%	1.56%	1.30%
MAX	8.96%	2.60%	1.44%	1.46%	1.62%	0.85%	6.77%	3.64%	2.35%
RMS	6.62%	1.43%	1.19%	0.41%	0.55%	0.25%	3.77%	1.81%	1.40%
MRE	6.73%	1.24%	1.18%	0.30%	0.47%	0.21%	3.28%	1.57%	1.28%
	Uncontrolled core								
	Category 1 inner			Category 2			Category 1 outer		
	SB	RN	LS	SB	RN	LS	SB	RN	LS
AVG	6.39%	1.10%	1.20%	0.46%	0.70%	0.21%	6.36%	1.31%	1.25%
MAX	8.95%	2.59%	1.50%	1.41%	1.56%	0.79%	8.93%	2.54%	1.76%
RMS	6.58%	1.43%	1.21%	0.58%	0.77%	0.28%	6.57%	1.49%	1.27%
MRE	6.66%	1.25%	1.20%	0.46%	0.70%	0.21%	6.60%	1.41%	1.22%

* SB: single block calculation; RN: renormalized spectra; LS: least square fitted spectra

CHAPTER 5
PBR TEST PROBLEM

5.1 Problem Description

The layout of a 2D PBR problem with azimuthal symmetry is shown in Figure 5.1. Multi-group cross sections are generated in each axial region (strip), from center to periphery: 2 inner reflector regions, 5 fuel regions, one outer reflector regions, one controlled region in which reflector and control rods are homogenized, and 2 outer reflector regions. Axially, the core is divided into 40 equal segments. From top to bottom of the core, the segments on the fuel-outer reflector interface are numbered as segment 1 to segment 40. The energy spectra are reconstructed on the interface for comparison to the reference spectra in each segment. The detailed specification for this benchmark problem can be found in Zhang et al (2010). The coarse-group (4G) and fine-group structures (33G and 71G) are presented in Table B.2 in Appendix B.

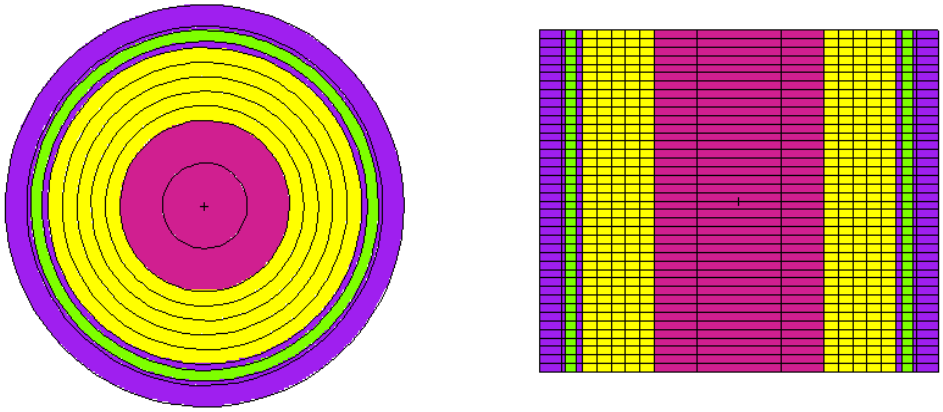

Figure 5.1. Layout of the PBR test problem with azimuthal symmetry

5.2 Reconstructed Energy Spectrum

Using the ESR methods of section 2.2, the scalar fluxes and net currents are reconstructed for each segment on the interface between the fuel region and the outer reflector region. For testing purpose, coarse group fluxes and net currents are calculated for each segment on the fuel-outer reflector interface in a whole core MCNP multi-group (33G) calculation. The MCNP calculation also tallies the reference fine group spectra (scalar flux and net current) for each segment. The "typical" spectrum is defined as the spatial average of reference fine group spectra, and is used together with a coarse group spectrum in the ESR methods for constructing the corresponding fine group spectrum. Two fine group structures, 33G and 71G, are used to test the ESR methods.

Similar to the HTR test problem, the collective errors are summarized for the reconstructed spectra for all 40 segments in the PBR test problem. From Table 5.1, it is found that the renormalized spectra agree very well with the reference spectra. However, the least-square fitted spectra are not as good as the renormalized spectra.

The energy spectrum reconstruction is performed again with a 71G structure. The collective errors are presented in Table 5.2. The least square fitted spectra are better than 33G results, but still not as good as the renormalized spectra. Based on this observation we do not recommend using the least square fitting method in PBR calculations.

Table 5.1. Collective errors in reconstructed energy spectra for PBR problem (33G)

		AVG	MAX	RMS	MRE
Scalar flux	RN	0.17%	1.95%	0.44%	0.17%
	LS	2.87%	4.00%	2.88%	2.87%
Net current	RN	0.61%	5.84%	1.31%	0.57%
	LS	6.57%	9.75%	6.61%	6.55%

* RN: renormalized spectra; LS: least square fitted spectra

Table 5.2. Collective errors in reconstructed energy spectra for PBR problem (71G)

		AVG	MAX	RMS	MRE
Scalar flux	RN	0.24%	2.16%	0.51%	0.24%
	LS	1.31%	2.84%	1.35%	1.31%
Net current	RN	1.07%	6.23%	1.60%	1.02%
	LS	2.47%	6.71%	2.65%	2.44%

* RN: renormalized spectra; LS: least square fitted spectra

CHAPTER 6
CONLCUSIONS

Two energy spectrum reconstruction methods have been developed in this thesis. It is assumed that there exists a “typical” fine group spectrum representing the core environment energy spectra. The renormalization method obtains the reconstructed spectra by renormalizing the “typical” spectrum so that it preserves the coarse group fluxes from the whole core diffusion calculation. The least square fitting method reconstructs a continuous energy spectrum, which can be expanded by B-spline bases, by minimizing its distance to the renormalized spectrum. The reconstructed spectrum can be then used in a local fine group transport calculation imbedded in whole core coarse group methods to improve the accuracy of the results by accounting for spectral effects, particularly, in regions near reflectors.

In the prismatic HTR problem, ESR methods are used to correct the absorption cross sections of BP pins. For BPs neighboring reflector or control rods, as compared with the single block results, the ESR methods reduce the MREs in energy spectra from 28% to less than 3%, and the MREs in the absorption rates from 7% to less than 1.5%. Renormalized spectra have the same accuracy as the least square fitted spectra. Therefore, it is recommended to use the renormalization method since it is easier to implement than the least square fitting method.

In the case of the PBR problem, the renormalized method is more accurate than the least square fitting method.

In summary, the ESR methods could reconstruct fine-group (or continuous energy) spectra from coarse group results based on “typical” energy spectra accurately. These reconstructed spectra can be used in on-the-fly local transport problems to improve the whole-core coarse-group diffusion solutions. In both prismatic HTR and PBR test problem, renormalization method consistently performs well in energy spectra reconstruction, and it is recommended for both cases. If continuous energy spectra are needed, least square fitting method is necessary although it maybe not as accurate as renormalization method in some cases.

APPENDIX A

B-SPLINE BASES

The set of fine-group boundaries E_h composes an ascending sequence $\{E_H, E_{H-1}, ...E_1, E_0\}$.Because the energy group widths vary up to several orders of magnitude, $\ln(E_h)$ is more suitable to act as the knots for B-spline bases. Therefore, $w = \ln(E)$ is used as the independent variable for the spline to reconstruct the energy spectrum.

Given the logarithms of energy group boundaries $w_h = \ln(E_h)$, for a spline space of degree *p*, a simple and commonly used approach to selecting knots is setting the first *p* knots identically equal to w_H and the last *p* knot identically equal to w_0. In other words, knot t_i is defined by

$$t_i = \begin{cases} w_H, 1 \le i \le p+1 \\ w_{H+p+1-i,} \; p+1 \le i \le H+p+1 \\ w_0, H+p+1 \le i \le H+2p+1 \end{cases}$$

According to de Boor (2001) and Siewer (2008), the *i*th B-spline basis of *p* degree can be recursively constructed by

$$B_{i,0}(w) = \begin{cases} 1, t_i \le w < t_{i+1} \\ 0, otherwise \end{cases}$$

$$B_{i,p}(w) = \frac{w - t_i}{t_{i+p} - t_i} B_{i,p-1}(w) + \frac{t_{i+p+1} - w}{t_{i+p+1} - t_{i+1}} B_{i+1,p-1}(w)$$

The degree *p* of B-spline space is pre-selected. In this research cubic spline is used, i.e. *p*=3. Figure A.1 presented an example of the bases of the cubic spline space based on 71 group boundaries.

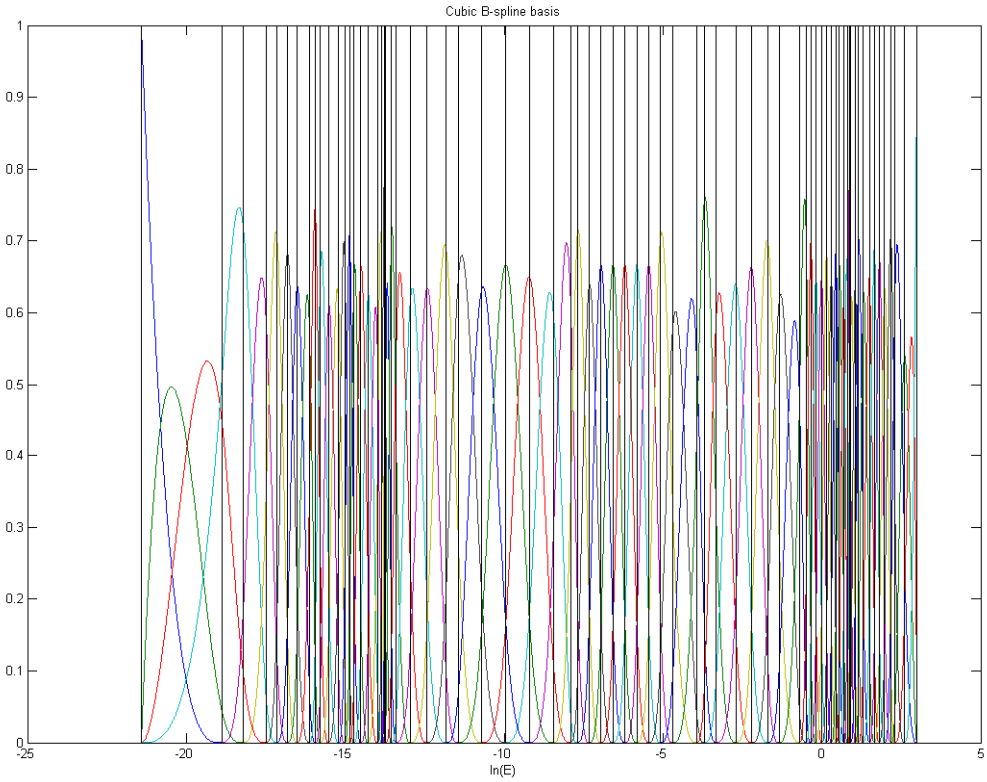

Figure A.1. Cubic B-spline bases

APPENDIX B

GROUP BOUNDARIES

Table B.1. Upper boundaries of energy group structures in the HTR test problem

Group Bdry	71G	30G	7G	Group Bdry	71G	30G	7G	Group Bdry	71G	30G	7G
2.00000E+01	1	1	1	2.59910E-01	25			2.38000E-06	49	13	
1.33800E+01	2			1.83200E-01	26	5		1.50000E-06	50	14	
1.00000E+01	3			1.11000E-01	27	6		1.30000E-06	51	15	
8.82500E+00	4			6.73800E-02	28	7		1.09700E-06	52	16	5
7.20000E+00	5			3.60660E-02	29			1.04500E-06	53	17	
6.06530E+00	6			2.47900E-02	30	8		9.72000E-07	54	18	
5.22050E+00	7			1.93050E-02	31			8.50000E-07	55	19	
4.49330E+00	8			9.11800E-03	32	9	3	6.25000E-07	56	20	
3.67900E+00	9	2		6.26730E-03	33			5.00000E-07	57	21	6
3.16640E+00	10			4.30740E-03	34			4.00000E-07	58	22	
2.86500E+00	11			2.96040E-03	35			3.50000E-07	59	23	
2.46600E+00	12			2.03470E-03	36			3.00000E-07	60	24	
2.36500E+00	13			1.39840E-03	37			2.50000E-07	61	25	
2.23130E+00	14			9.61120E-04	38			1.80000E-07	62	26	
2.01890E+00	15			6.60570E-04	39			1.40000E-07	63	27	
1.73770E+00	16			4.54000E-04	40	10		1.20000E-07	64	28	
1.57240E+00	17			3.67300E-04	41	11		1.00000E-07	65	29	7
1.35300E+00	18	3		2.14450E-04	42			6.70000E-08	66		
1.16490E+00	19			1.01300E-04	43			5.00000E-08	67	30	
1.00260E+00	20			4.78510E-05	44			3.55000E-08	68		
8.20850E-01	21			2.26030E-05	45			2.55000E-08	69		
7.06510E-01	22			1.06770E-05	46			1.23960E-08	70		
6.08100E-01	23			7.33820E-06	47			6.32470E-09	71		
5.00000E-01	24	4	2	4.00000E-06	48	12	4				

Table B.2. Upper boundaries of energy group structures in the PBR test problem

Group Boundary	71G	33G	4G	Group Boundary	71G	33G	4G	Group Boundary	71G	33G	4G
2.00000E+01	1	1	1	2.59910E-01	25			2.38000E-06	49	13	
1.33800E+01	2			1.83200E-01	26	5		1.50000E-06	50	14	
1.00000E+01	3			1.11000E-01	27	6		1.30000E-06	51	15	
8.82500E+00	4			6.73800E-02	28	7		1.09700E-06	52	16	
7.20000E+00	5			3.60660E-02	29			1.04500E-06	53	17	
6.06530E+00	6			2.47900E-02	30	8		9.72000E-07	54	18	
5.22050E+00	7			1.93050E-02	31			8.50000E-07	55	19	
4.49330E+00	8			9.11800E-03	32	9	2	6.25000E-07	56	20	
3.67900E+00	9	2		6.26730E-03	33			5.00000E-07	57	21	3
3.16640E+00	10			4.30740E-03	34			4.00000E-07	58		
2.86500E+00	11			2.96040E-03	35			3.50000E-07	59	22	
2.46600E+00	12			2.03470E-03	36			3.00000E-07	60	23	
2.36500E+00	13			1.39840E-03	37			2.50000E-07	61	24	
2.23130E+00	14			9.61120E-04	38			1.80000E-07	62	25	
2.01890E+00	15			6.60570E-04	39			1.40000E-07	63	26	
1.73770E+00	16			4.54000E-04	40	10		1.20000E-07	64	27	
1.57240E+00	17			3.67300E-04	41	11		1.00000E-07	65	28	4
1.35300E+00	18	3		2.14450E-04	42			6.70000E-08	66	29	
1.16490E+00	19			1.01300E-04	43			5.00000E-08	67	30	
1.00260E+00	20			4.78510E-05	44			3.55000E-08	68	31	
8.20850E-01	21			2.26030E-05	45			2.55000E-08	69		
7.06510E-01	22			1.06770E-05	46			1.23960E-08	70	32	
6.08100E-01	23			7.33820E-06	47			6.32470E-09	71	33	
5.00000E-01	24	4		4.00000E-06	48	12					

APPENDIX C

COLLECTIVE ERROR DEFINATION

The following statistics are used to represent the collective errors for a set containing N elements $\{x_1, x_2, \text{L}\ x_N\}$ with errors of $\{e_1, e_2, \text{L}\ e_N\}$ respectively.

Average error (AVG):

$$AVG = \frac{\sum_{N} |e_n|}{N}$$

Maximum error(MAX):

$$MAX = \max(|e_n|)$$

Root-mean-square average error (RMS):

$$RMS = \sqrt{\frac{\sum_{N} e_n^2}{N}}$$

Mean relative error (MRE):

$$MRE = \frac{\sum_{N} |e_n| \cdot x_n}{N \cdot x_{avg}}$$

APPENDIX D

BP ABSORPTION CROSS SECTION ERRORS IN THE HTR PROBLEM

Table D.1. Absorption cross sections and errors in fuel block 4 of the controlled core

	Reference BP absorption cross sections					
	Pin 1	Pin 2	Pin 3	Pin 4	Pin 5	Pin 6
G7 XS*	4.8094E-01	4.9690E-01	4.8153E-01	4.5723E-01	4.5167E-01	4.5621E-01
G6 XS	2.3054E-01	2.3702E-01	2.3045E-01	2.2426E-01	2.2292E-01	2.2420E-01
G5 XS	1.1358E-01	1.1366E-01	1.1365E-01	1.1357E-01	1.1360E-01	1.1362E-01
G4 XS	6.8075E-02	6.8169E-02	6.8022E-02	6.7901E-02	6.7986E-02	6.7959E-02
G3 XS	1.0953E-02	1.1367E-02	1.0949E-02	1.0744E-02	1.0809E-02	1.0756E-02
G2 XS	4.1012E-04	4.0793E-04	4.1122E-04	4.1382E-04	4.1626E-04	4.1431E-04
G1 XS	8.6763E-05	8.8243E-05	8.6625E-05	8.5106E-05	8.4599E-05	8.4673E-05
Ab. Rates**	4.4911E-04	6.4615E-04	4.5304E-04	2.9371E-04	2.6767E-04	2.9208E-04
	Errors in absorption cross sections generated in single block calculation					
G7 XS	-7.04%	-10.02%	-7.15%	-2.22%	-1.01%	-2.00%
G6 XS	-3.53%	-6.16%	-3.49%	-0.83%	-0.23%	-0.80%
G5 XS	0.02%	-0.05%	-0.04%	0.03%	0.00%	-0.02%
G4 XS	-0.10%	-0.24%	-0.02%	0.16%	0.03%	0.07%
G3 XS	1.03%	-2.65%	1.07%	2.99%	2.38%	2.89%
G2 XS	2.03%	2.58%	1.76%	1.12%	0.53%	1.00%
G1 XS	-2.06%	-3.70%	-1.90%	-0.15%	0.45%	0.36%
Ab. rates	-5.68%	-8.96%	-5.75%	-1.34%	-0.47%	-1.20%
	Errors in absorption cross sections generated by renormalized spectra					
G7 XS	0.48%	-2.67%	0.35%	-1.90%	-0.73%	-1.69%
G6 XS	-0.05%	-2.55%	-0.01%	-1.27%	-0.72%	-1.25%
G5 XS	-0.18%	-0.22%	-0.24%	-0.22%	-0.25%	-0.26%
G4 XS	-0.61%	-0.64%	-0.53%	-0.50%	-0.62%	-0.58%
G3 XS	-0.33%	-3.93%	-0.29%	-0.42%	-0.98%	-0.52%
G2 XS	-0.76%	-0.29%	-1.01%	-0.25%	-0.82%	-0.38%
G1 XS	1.34%	-0.36%	1.50%	1.01%	1.62%	1.53%
Ab. rates	0.30%	-2.60%	0.22%	-1.51%	-0.71%	-1.39%

* G7 XS: Group7 absorption cross section

** Ab. Rate: absorption rates

Table D.1.(continued) Absorption cross sections and errors in fuel block 4 of the controlled core

	Errors in absorption cross sections generated by least square fitted spectra					
G7 XS	1.50%	-1.15%	1.39%	-0.65%	0.30%	-0.47%
G6 XS	-0.17%	-2.11%	-0.13%	-1.21%	-0.78%	-1.21%
G5 XS	-0.21%	-0.16%	-0.27%	-0.21%	-0.25%	-0.25%
G4 XS	-0.62%	-0.57%	-0.54%	-0.50%	-0.61%	-0.57%
G3 XS	-0.29%	-3.71%	-0.24%	-0.36%	-0.89%	-0.45%
G2 XS	-0.77%	-0.30%	-1.01%	-0.30%	-0.83%	-0.42%
G1 XS	5.75%	5.44%	5.59%	5.76%	5.97%	6.39%
Ab. rates	1.00%	-1.32%	0.93%	-0.75%	-0.16%	-0.66%
	Errors in absorption cross sections generated by reference spectra					
G7 XS	-0.61%	-0.67%	-0.63%	-0.41%	-0.39%	-0.40%
G6 XS	-0.62%	-0.72%	-0.66%	-0.59%	-0.50%	-0.61%
G5 XS	-0.22%	-0.21%	-0.26%	-0.22%	-0.25%	-0.26%
G4 XS	-0.67%	-0.61%	-0.52%	-0.51%	-0.64%	-0.54%
G3 XS	-1.22%	-1.38%	-1.30%	-1.19%	-1.05%	-1.14%
G2 XS	-0.76%	-0.74%	-0.75%	-0.77%	-0.78%	-0.82%
G1 XS	0.96%	2.13%	0.94%	1.39%	1.40%	1.12%
Ab. rates	-0.62%	-0.68%	-0.65%	-0.50%	-0.47%	-0.50%

Table D.2. Collective errors in absorption cross sections and absorption rates of BP pins in three BP categories in the controlled core

		Category 1				Category 2				Category 3			
		SB	ref	RN	LS	SB	ref	RN	LS	SB	ref	RN	LS
AVG	G7 XS	7.72%	0.62%	1.24%	1.50%	0.53%	0.35%	0.39%	0.72%	4.35%	0.49%	2.06%	1.92%
	G6 XS	4.10%	0.64%	0.85%	0.71%	0.21%	0.56%	0.53%	0.64%	1.68%	0.59%	0.89%	0.75%
	G5 XS	0.05%	0.23%	0.23%	0.23%	0.03%	0.22%	0.22%	0.22%	0.04%	0.23%	0.23%	0.22%
	G4 XS	0.09%	0.57%	0.57%	0.56%	0.07%	0.57%	0.57%	0.56%	0.08%	0.57%	0.58%	0.56%
	G3 XS	1.40%	1.28%	1.50%	1.40%	2.08%	1.18%	1.28%	1.18%	1.36%	1.25%	1.50%	1.40%
	G2 XS	2.02%	0.81%	0.78%	0.78%	0.53%	0.79%	0.82%	0.82%	0.35%	0.79%	0.79%	0.79%
	G1 XS	2.50%	0.97%	1.37%	5.55%	0.45%	1.13%	1.10%	5.41%	1.29%	1.69%	1.46%	5.62%
	Ab. rate	6.43%	0.63%	1.07%	1.18%	0.25%	0.47%	0.43%	0.20%	3.21%	0.55%	1.56%	1.30%
MAX	G7 XS	10.02%	0.72%	2.67%	2.08%	2.35%	0.47%	2.03%	1.02%	8.07%	0.70%	4.00%	2.62%
	G6 XS	6.16%	0.72%	2.55%	2.11%	0.85%	0.69%	1.29%	1.23%	4.02%	0.75%	2.86%	2.42%
	G5 XS	0.13%	0.31%	0.31%	0.29%	0.09%	0.28%	0.28%	0.29%	0.09%	0.31%	0.30%	0.29%
	G4 XS	0.24%	0.67%	0.65%	0.62%	0.16%	0.67%	0.68%	0.67%	0.21%	0.70%	0.69%	0.69%
	G3 XS	2.77%	1.49%	4.04%	3.81%	3.64%	1.37%	2.17%	2.03%	3.40%	1.44%	5.10%	4.83%
	G2 XS	2.59%	0.90%	1.29%	1.26%	1.12%	1.01%	1.12%	1.10%	1.05%	0.98%	1.46%	1.41%
	G1 XS	4.46%	2.13%	2.63%	6.90%	1.24%	2.50%	2.18%	6.79%	3.79%	6.58%	3.39%	8.57%
	Ab. rate	8.96%	0.71%	2.60%	1.44%	1.46%	0.54%	1.62%	0.85%	6.77%	0.67%	3.64%	2.35%
RMS	G7 XS	7.86%	0.62%	1.54%	1.54%	0.77%	0.35%	0.61%	0.78%	4.88%	0.50%	2.26%	2.04%
	G6 XS	4.29%	0.65%	1.35%	1.11%	0.28%	0.56%	0.59%	0.67%	2.04%	0.60%	1.27%	1.10%
	G5 XS	0.06%	0.23%	0.23%	0.23%	0.04%	0.22%	0.22%	0.23%	0.05%	0.23%	0.23%	0.23%
	G4 XS	0.12%	0.57%	0.58%	0.56%	0.08%	0.57%	0.57%	0.56%	0.10%	0.58%	0.58%	0.57%
	G3 XS	1.65%	1.29%	2.15%	2.02%	2.19%	1.18%	1.42%	1.32%	1.61%	1.26%	2.10%	1.97%
	G2 XS	2.05%	0.82%	0.84%	0.84%	0.58%	0.80%	0.85%	0.84%	0.48%	0.80%	0.89%	0.89%
	G1 XS	2.77%	1.11%	1.51%	5.60%	0.55%	1.27%	1.23%	5.45%	1.60%	2.10%	1.75%	5.80%
	Ab. rate	6.62%	0.63%	1.43%	1.19%	0.41%	0.47%	0.55%	0.25%	3.77%	0.55%	1.81%	1.40%
MRE	G7 XS	7.74%	0.62%	1.25%	1.50%	0.53%	0.35%	0.39%	0.72%	4.41%	0.49%	2.08%	1.92%
	G6 XS	4.11%	0.64%	0.86%	0.72%	0.21%	0.56%	0.53%	0.64%	1.69%	0.59%	0.90%	0.76%
	G5 XS	0.05%	0.23%	0.23%	0.23%	0.03%	0.22%	0.22%	0.22%	0.04%	0.23%	0.23%	0.22%
	G4 XS	0.09%	0.57%	0.57%	0.56%	0.07%	0.57%	0.57%	0.56%	0.08%	0.57%	0.58%	0.56%
	G3 XS	1.41%	1.28%	1.52%	1.43%	2.08%	1.18%	1.28%	1.18%	1.36%	1.25%	1.53%	1.42%
	G2 XS	2.02%	0.81%	0.78%	0.78%	0.53%	0.79%	0.82%	0.82%	0.35%	0.79%	0.79%	0.80%
	G1 XS	2.51%	0.96%	1.37%	5.54%	0.45%	1.12%	1.10%	5.41%	1.30%	1.68%	1.45%	5.61%
	Ab. rate	6.73%	0.63%	1.24%	1.18%	0.30%	0.47%	0.47%	0.21%	3.28%	0.55%	1.57%	1.28%

* SB: single block calculation; Ref: reference energy spectra; RN: renormalized spectra; LS: least square fitted spectra

Table D.3. Absorption cross sections and errors in fuel block 4 of the uncontrolled core

	Reference BP absorption cross sections					
	Pin 1	Pin 2	Pin 3	Pin 4	Pin 5	Pin 6
G7 XS	4.8057E-01	4.9674E-01	4.8062E-01	4.5689E-01	4.5143E-01	4.5579E-01
G6 XS	2.3055E-01	2.3710E-01	2.3046E-01	2.2444E-01	2.2303E-01	2.2429E-01
G5 XS	1.1362E-01	1.1367E-01	1.1367E-01	1.1366E-01	1.1362E-01	1.1356E-01
G4 XS	6.8061E-02	6.8189E-02	6.8030E-02	6.7939E-02	6.7985E-02	6.7971E-02
G3 XS	1.1043E-02	1.1417E-02	1.1047E-02	1.0848E-02	1.0906E-02	1.0884E-02
G2 XS	4.1100E-04	4.0921E-04	4.1232E-04	4.1492E-04	4.1755E-04	4.1510E-04
G1 XS	8.7411E-05	8.8929E-05	8.6742E-05	8.5220E-05	8.4772E-05	8.6152E-05
Ab. rates	3.4962E-04	4.9656E-04	3.5569E-04	2.4273E-04	2.2974E-04	2.4067E-04
	Errors in absorption cross sections generated in single block calculation					
G7 XS	-6.96%	-9.99%	-6.97%	-2.14%	-0.96%	-1.91%
G6 XS	-3.53%	-6.20%	-3.49%	-0.91%	-0.28%	-0.84%
G5 XS	-0.02%	-0.06%	-0.05%	-0.05%	-0.01%	0.04%
G4 XS	-0.08%	-0.26%	-0.03%	0.10%	0.03%	0.05%
G3 XS	0.21%	-3.08%	0.17%	2.02%	1.47%	1.68%
G2 XS	1.82%	2.26%	1.49%	0.85%	0.22%	0.81%
G1 XS	-2.79%	-4.44%	-2.04%	-0.29%	0.24%	-1.36%
Ab. rates	-5.66%	-8.95%	-5.66%	-1.38%	-0.52%	-1.24%
	Errors in absorption cross sections generated by renormalized spectra					
G7 XS	0.44%	-2.75%	0.43%	-1.57%	-0.41%	-1.33%
G6 XS	-0.06%	-2.60%	-0.02%	-1.14%	-0.56%	-1.08%
G5 XS	-0.19%	-0.20%	-0.23%	-0.29%	-0.25%	-0.20%
G4 XS	-0.58%	-0.66%	-0.53%	-0.52%	-0.58%	-0.56%
G3 XS	-0.36%	-3.59%	-0.39%	-1.04%	-1.54%	-1.37%
G2 XS	-0.66%	-0.29%	-0.97%	-0.38%	-0.99%	-0.42%
G1 XS	0.19%	-1.52%	0.96%	0.59%	1.13%	-0.49%
Ab. rates	0.27%	-2.66%	0.27%	-1.32%	-0.52%	-1.18%
	Errors in absorption cross sections generated by least square fitted spectra					
G7 XS	1.58%	-1.12%	1.56%	-0.58%	0.35%	-0.38%
G6 XS	-0.17%	-2.15%	-0.13%	-1.29%	-0.82%	-1.24%
G5 XS	-0.23%	-0.16%	-0.27%	-0.28%	-0.25%	-0.19%
G4 XS	-0.57%	-0.57%	-0.52%	-0.51%	-0.57%	-0.54%
G3 XS	-1.04%	-4.08%	-1.06%	-1.24%	-1.70%	-1.54%
G2 XS	-0.94%	-0.57%	-1.24%	-0.53%	-1.10%	-0.57%
G1 XS	4.64%	4.44%	5.20%	5.43%	5.49%	4.35%
Ab. rates	1.04%	-1.31%	1.03%	-0.79%	-0.18%	-0.67%

* G7 XS: Group7 absorption cross section

** Ab. Rate: absorption rates

Table D.3.(continued) Absorption cross sections and errors in fuel block 4 of the uncontrolled core

	Errors in absorption cross sections generated by reference spectra					
G7 XS	-0.60%	-0.65%	-0.64%	-0.40%	-0.36%	-0.44%
G6 XS	-0.72%	-0.68%	-0.62%	-0.63%	-0.56%	-0.63%
G5 XS	-0.18%	-0.14%	-0.19%	-0.23%	-0.28%	-0.18%
G4 XS	-0.55%	-0.67%	-0.52%	-0.51%	-0.59%	-0.50%
G3 XS	-1.33%	-1.36%	-1.19%	-1.39%	-1.13%	-1.27%
G2 XS	-0.64%	-0.75%	-0.77%	-0.85%	-0.85%	-0.74%
G1 XS	0.33%	0.19%	-0.14%	0.60%	1.54%	0.35%
Ab. rates	-0.64%	-0.66%	-0.64%	-0.52%	-0.47%	-0.53%

Table D.4. Collective errors in absorption cross sections and absorption rates of BP pins in three BP categories in the uncontrolled core

		Category 1 inner				Category 2				Category 1 outer			
		SB	ref	RN	LS	SB	ref	RN	LS	SB	ref	RN	LS
AVG	G7 XS	7.62%	0.61%	1.31%	1.57%	0.89%	0.36%	0.60%	0.49%	7.57%	0.61%	1.53%	1.58%
	G6 XS	4.12%	0.65%	0.87%	0.73%	0.30%	0.56%	0.77%	0.83%	4.12%	0.64%	1.05%	0.80%
	G5 XS	0.04%	0.19%	0.22%	0.22%	0.03%	0.22%	0.23%	0.22%	0.05%	0.22%	0.24%	0.24%
	G4 XS	0.10%	0.57%	0.57%	0.54%	0.06%	0.57%	0.58%	0.56%	0.12%	0.57%	0.58%	0.55%
	G3 XS	1.22%	1.34%	2.23%	2.09%	1.82%	1.22%	1.51%	1.40%	1.41%	1.31%	2.18%	2.04%
	G2 XS	1.72%	0.80%	1.06%	1.03%	0.42%	0.79%	0.92%	0.91%	1.76%	0.80%	1.02%	1.00%
	G1 XS	2.33%	0.88%	1.59%	5.42%	0.56%	1.00%	1.21%	5.32%	2.17%	1.12%	1.72%	5.66%
	Ab. rate	6.39%	0.63%	1.10%	1.20%	0.46%	0.47%	0.70%	0.21%	6.36%	0.62%	1.31%	1.25%
MAX	G7 XS	9.99%	0.69%	2.64%	2.21%	2.14%	0.49%	1.83%	0.88%	9.92%	0.67%	2.56%	2.55%
	G6 XS	6.20%	0.72%	2.59%	2.15%	0.92%	0.64%	1.35%	1.29%	6.40%	0.72%	2.78%	2.32%
	G5 XS	0.08%	0.28%	0.25%	0.29%	0.08%	0.30%	0.30%	0.30%	0.15%	0.28%	0.32%	0.30%
	G4 XS	0.30%	0.67%	0.69%	0.60%	0.15%	0.64%	0.67%	0.66%	0.25%	0.65%	0.66%	0.66%
	G3 XS	3.57%	1.59%	4.82%	4.55%	2.61%	1.42%	2.07%	1.91%	3.58%	1.61%	4.81%	4.53%
	G2 XS	2.26%	0.89%	1.56%	1.50%	0.85%	1.00%	1.28%	1.25%	2.74%	0.94%	1.75%	1.68%
	G1 XS	4.84%	1.81%	3.01%	7.25%	1.66%	2.38%	2.19%	6.74%	4.83%	2.29%	3.95%	7.54%
	Ab. rate	8.95%	0.68%	2.59%	1.50%	1.41%	0.56%	1.56%	0.79%	8.93%	0.67%	2.54%	1.76%
RMS	G7 XS	7.76%	0.61%	1.55%	1.62%	1.02%	0.36%	0.78%	0.56%	7.73%	0.61%	1.64%	1.71%
	G6 XS	4.31%	0.66%	1.37%	1.13%	0.39%	0.57%	0.81%	0.85%	4.33%	0.64%	1.42%	1.17%
	G5 XS	0.05%	0.20%	0.22%	0.22%	0.03%	0.22%	0.23%	0.22%	0.06%	0.22%	0.24%	0.24%
	G4 XS	0.14%	0.57%	0.57%	0.54%	0.07%	0.57%	0.58%	0.57%	0.15%	0.58%	0.58%	0.55%
	G3 XS	1.81%	1.34%	2.70%	2.54%	1.86%	1.23%	1.55%	1.43%	1.86%	1.31%	2.71%	2.54%
	G2 XS	1.76%	0.80%	1.11%	1.08%	0.49%	0.80%	0.95%	0.94%	1.83%	0.80%	1.11%	1.08%
	G1 XS	2.69%	1.08%	1.73%	5.49%	0.67%	1.16%	1.34%	5.37%	2.58%	1.30%	2.02%	5.75%
	Ab. rate	6.58%	0.63%	1.43%	1.21%	0.58%	0.48%	0.77%	0.28%	6.57%	0.63%	1.49%	1.27%
MRE	G7 XS	7.64%	0.61%	1.32%	1.56%	0.89%	0.36%	0.61%	0.49%	7.60%	0.61%	1.54%	1.57%
	G6 XS	4.13%	0.65%	0.88%	0.74%	0.30%	0.56%	0.77%	0.83%	4.14%	0.64%	1.06%	0.81%
	G5 XS	0.04%	0.19%	0.22%	0.22%	0.03%	0.22%	0.23%	0.22%	0.05%	0.22%	0.24%	0.24%
	G4 XS	0.10%	0.57%	0.57%	0.54%	0.06%	0.57%	0.58%	0.56%	0.12%	0.57%	0.58%	0.55%
	G3 XS	1.24%	1.34%	2.25%	2.11%	1.82%	1.22%	1.51%	1.40%	1.42%	1.31%	2.21%	2.07%
	G2 XS	1.72%	0.80%	1.06%	1.04%	0.42%	0.79%	0.92%	0.91%	1.76%	0.80%	1.02%	1.00%
	G1 XS	2.35%	0.88%	1.59%	5.41%	0.56%	1.00%	1.20%	5.32%	2.19%	1.12%	1.71%	5.65%
	Ab. rate	6.66%	0.63%	1.25%	1.20%	0.46%	0.47%	0.70%	0.21%	6.60%	0.63%	1.41%	1.22%

* SB: single block calculation; Ref: reference energy spectra; RN: renormalized spectra; LS: least square fitted spectra

REFERENCES

de Boor, C. A Practical Guide to Splines, Revised Edition, New York: Springer, (2001)

Forget, B., Rahnema, F., and Mosher, S. "A Heterogeneous coarse Mesh Solution for the 2-D MOX Benchmark Problem," Prog. Nucl. Energy, 45, No. 2-4, 233-254. (2004)

Lee, C.H., Zhong, Z., Taiwo, T.A., Yang, W. S., Smith, M.A., and Palmiotti G., "Status of Reactor Physics Activities on Cross Section Generation and Functionalization for the Prismatic Very High Temperature Reactor, and Development of Spatially-Heterogeneous Codes", *ANL-GenIV-075*, (2006)

Siewer, R., "Histopolating Splines", Journal of Computational and Applied Mathematics, vol. 220, pp. 661-673, (2008).

Sterberntz, J. W., Phillips, B., Sant, R. L, Chang, G. S., and Bayless P.D , "Reactor Physics Parametric and Depletion Studies in Support of TRISO Particle Fuel Specification for the Next Generation Nuclear Plant", Idaho National Engineering and Environmental Laboratory, INEEL/EXT-04-02331.(2004)

X-5 Monte Carlo Team, MCNP – A General Monte Carlo N-Particle Transport Code, Version 5. Los Alamos National Laboratory, LA-CP-03-0245. (2003)

Zhang, D., Rahnema, F., Ougouag, A. M., and Gleicher, F., "Local Response-Function-Based Transport Method for Diffusion-Transport Hybrid Calculations in Pebble Bed Reactors," 5th International Conference on High Temperature Reactor Technology (HTR 2010), Prague, Czech Republic, October 18-20, (2010)